

# Mechanism and function of Vav1 localisation in TCR signalling

Olga Ksionda<sup>1,\*</sup>, Alexander Saveliev<sup>1,‡</sup>, Robert Köchl<sup>1</sup>, Jonathan Rapley<sup>1,2,§</sup>, Mustapha Faroudi<sup>1,¶</sup>, Jennifer E. Smith-Garvin<sup>4,\*\*</sup>, Christoph Wülfing<sup>5,†‡</sup>, Katrin Rittinger<sup>2</sup>, Tom Carter<sup>3</sup> and Victor L. J. Tybulewicz<sup>1,§§</sup>

<sup>1</sup>Division of Immune Cell Biology, MRC National Institute for Medical Research, London NW7 1AA, UK

<sup>2</sup>Division of Molecular Structure, MRC National Institute for Medical Research, London NW7 1AA, UK

<sup>3</sup>Division of Physical Biochemistry, MRC National Institute for Medical Research, London NW7 1AA, UK

<sup>4</sup>University of Pennsylvania School of Medicine, Philadelphia, PA 19104, USA

<sup>5</sup>UT Southwestern Medical Center, Dallas, TX 75390, USA

\*Present address: University of California, San Francisco, CA 94143, USA

‡Present address: Babraham Institute, Babraham Research Campus, Cambridge CB22 3AT, UK

§Present address: Fujifilm Diosynth Biotechnologies UK Ltd, Belasis Avenue, Billingham TS23 1LH, UK

¶Present address: Centre d'Immunologie Marseille Luminy, Marseille, France

\*\*Present address: Fox Chase Cancer Center, Philadelphia, PA 19111, USA

††Present address: University of Bristol, Bristol, BS8 1TD, UK

§§Author for correspondence ([vtybule@nimr.mrc.ac.uk](mailto:vtybule@nimr.mrc.ac.uk))

Accepted 8 August 2012

Journal of Cell Science 125, 5302–5314

© 2012. Published by The Company of Biologists Ltd

doi: 10.1242/jcs.105148

## Summary

The antigen-specific binding of T cells to antigen presenting cells results in recruitment of signalling proteins to microclusters at the cell-cell interface known as the immunological synapse (IS). The Vav1 guanine nucleotide exchange factor plays a critical role in T cell antigen receptor (TCR) signalling, leading to the activation of multiple pathways. We now show that it is recruited to microclusters and to the IS in primary CD4<sup>+</sup> and CD8<sup>+</sup> T cells. Furthermore, we show that this recruitment depends on the SH2 and C-terminal SH3 (SH3<sub>B</sub>) domains of Vav1, and on phosphotyrosines 112 and 128 of the SLP76 adaptor protein. Biophysical measurements show that Vav1 binds directly to these residues on SLP76 and that efficient binding depends on the SH2 and SH3<sub>B</sub> domains of Vav1. Finally, we show that the same two domains are critical for the phosphorylation of Vav1 and its signalling function in TCR-induced calcium flux. We propose that Vav1 is recruited to the IS by binding to SLP76 and that this interaction is critical for the transduction of signals leading to calcium flux.

**Key words:** Immunological synapse, T cell, Signal transduction, SLP76, Vav1

## Introduction

Antigen-specific activation of T cells is triggered by the binding of the cell surface T cell antigen receptor (TCR) to antigenic peptide bound to MHC molecules (pMHC) on the surface of an antigen-presenting cell (APC). Initial binding of pMHC to TCR results in signal transduction from the TCR, leading to activation of integrins, binding of these adhesion molecules to their counter-receptors on the APC and hence the formation of a stable T cell:APC conjugate. The cell-cell interface of this integrin-stabilised conjugate has been termed the immunological synapse (IS) (Dustin et al., 2010; Dustin et al., 1998). In some cases the IS is characterised by an ordered arrangement of proteins, with a central accumulation of TCR molecules surrounded by a ring of integrins in zones known as the central and peripheral supramolecular activation clusters (cSMAC and pSMAC) respectively (Monks et al., 1998). Imaging of signalling proteins has shown that these also segregate within the IS, with, for example, PKC $\theta$  and talin found in the cSMAC and

pSMAC respectively. Kinetic analysis of T cells interacting with pMHC and integrin ligands presented on supported lipid bilayers has shown that within seconds of ligand engagement, the TCR forms microclusters in the periphery of the IS which then move to the centre of the synapse over the course of several minutes to form the cSMAC (Campi et al., 2005; Grakoui et al., 1999; Yokosuka et al., 2005). Signalling molecules such as the ZAP70 kinase and the LAT and SLP76 adaptors are also recruited to microclusters within the IS, and these too migrate centripetally, though they dissociate before reaching the cSMAC (Yokosuka et al., 2005). Studies have shown that active signalling occurs in the peripheral microclusters, but is usually extinguished within the cSMAC, which may be an area from which TCR molecules are internalised (Campi et al., 2005; Grakoui et al., 1999; Mossman et al., 2005; Varma et al., 2006). TCR microclusters have also been observed in an alternative imaging system where T cells interact with antibodies to the TCR and, in some cases to CD28, immobilised on glass (Barda-Saad et al., 2005; Braiman et al., 2006; Bunnell et al., 2002; Bunnell et al., 2001). In these studies, the TCR microclusters form but are unable to move because they are bound by immobilised anti-CD3 antibodies, and thus the system is best used to study the initial TCR proximal signalling events (Bunnell et al., 2002; Bunnell et al., 2006).

Finally, live cell 3D imaging of 30 different signalling sensors in T cells conjugated to APCs has shown a diverse range of spatiotemporal patterning, which may be important for efficient T cell activation (Singleton et al., 2009).

Vav1 is a guanine nucleotide exchange factor (GEF) for Rho family GTPases (Tybulewicz, 2005), which plays an important role in TCR signalling, transducing signals that lead to an increase in intracellular  $Ca^{2+}$  (calcium flux), and the activation of

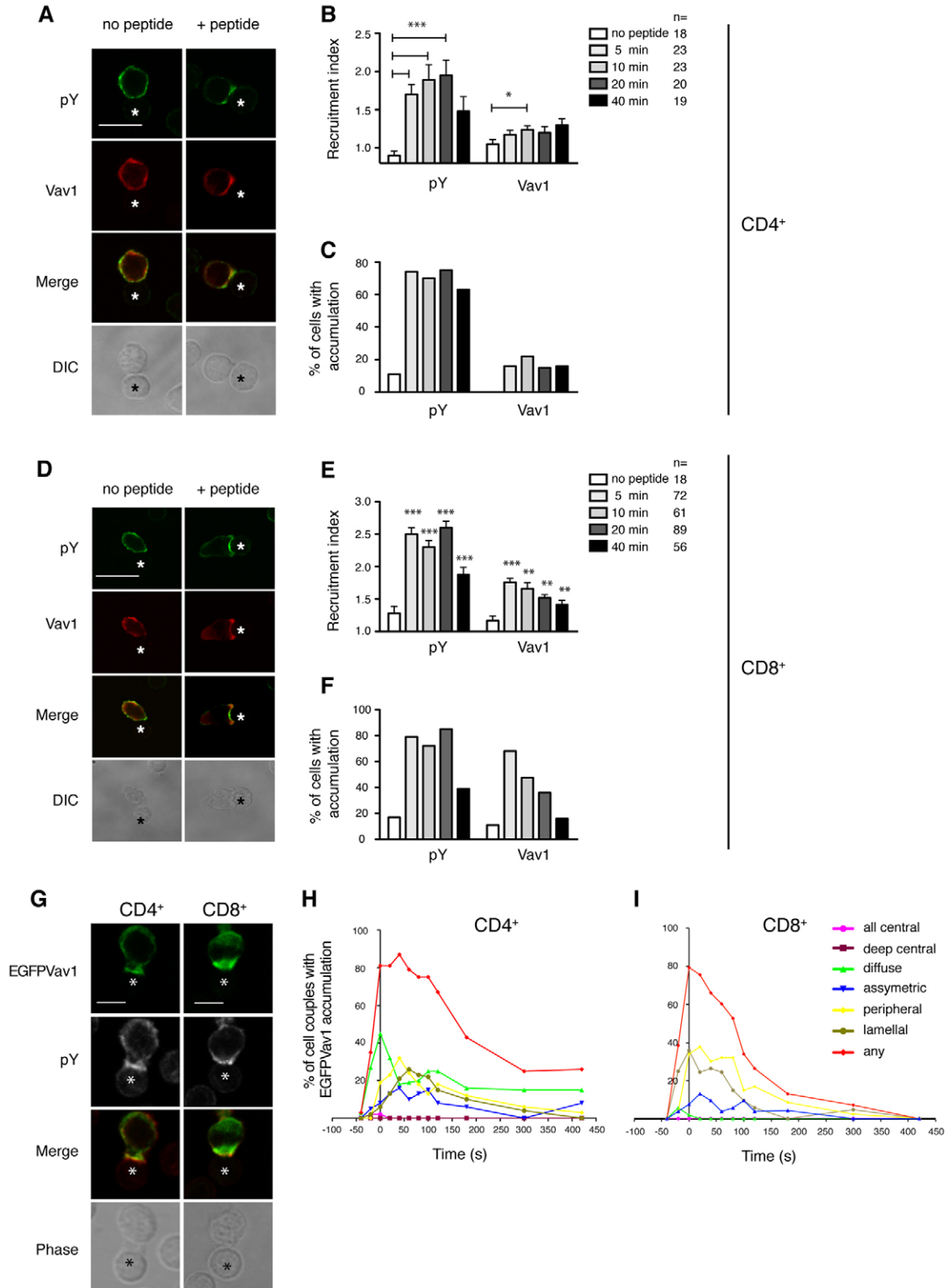


Fig. 1. See next page for legend.

ERK MAP kinases, phosphoinositide-3-kinase (PI3K), the Akt kinase, and the transcription factors nuclear factor  $\kappa$ B (NF- $\kappa$ B) and nuclear factor of activated T cells (NFAT) (Costello et al., 1999; Fischer et al., 1998; Holsinger et al., 1998; Reynolds et al., 2004; Reynolds et al., 2002; Tybulewicz, 2005). Vav1 is also required to transduce signals leading to integrin activation and cytoskeletal rearrangements, and cell polarisation (Ardouin et al., 2003; Fischer et al., 1998; Holsinger et al., 1998; Krawczyk et al., 2002; Wülfing et al., 2000).

Structural analysis of Vav1 has shown that it contains multiple domains (Fig. 2A). The GEF activity of Vav1 resides in the Dbl homology (DH) domain, which is tightly associated with pleckstrin homology (PH) and C1 domains, forming a catalytic core (Chrencik et al., 2008; Rapley et al., 2008). N-terminal to these are a calponin homology (CH) domain and an acidic region that negatively regulate the GEF activity of Vav1 by binding to the DH and PH domains and sterically blocking binding of the GTPase substrates (Aghazadeh et al., 2000; Yu et al., 2010). Phosphorylation of tyrosine residues located within the acidic domain leads to dissociation of the CH and acidic domains from the DH-PH-C1 catalytic core of Vav1 and hence increased enzymatic activity (Aghazadeh et al., 2000; Yu et al., 2010). C-terminal to the DH-PH-C1 domains of Vav1, the protein contains one SH2 domain and two SH3 domains (SH3<sub>A</sub>, SH3<sub>B</sub>), suggesting that Vav1 may function as an adaptor as well as a GEF. Recently we showed that the GEF activity of Vav1 is important for some but not all of its functions. In T cells expressing a GEF-deficient Vav1, TCR-induced activation of Rac1, Akt and integrins is defective (Saveliev et al., 2009). In contrast, TCR-induced calcium flux, ERK activation and cell polarisation are not affected by this GEF mutation, demonstrating that Vav1 has GEF-independent functions, potentially as an adaptor protein.

Vav1 has been reported to associate with a number of other signalling proteins in T cells (Tybulewicz, 2005). Through its

SH2 domain Vav1 can bind to phosphotyrosine (pY) 315 on the ZAP70 kinase, an interaction that may be required for subsequent phosphorylation of Vav1 by ZAP70 (Katzav et al., 1994; Wu et al., 1997). Additionally, the SH2 domain of Vav1 has been reported to bind phosphotyrosine pY112 and pY128 of SLP76 (numbering given for mouse SLP76, corresponding to Y113 and Y128 in human SLP76), an adaptor protein critical for TCR signalling (Fang and Koretzky, 1999; Koretzky et al., 2006; Tuosto et al., 1996; Wu et al., 1996). The SH3<sub>A</sub> domain of Vav1 can bind to an SH3 domain of the Grb2 adaptor protein through an atypical SH3-SH3 interaction (Nishida et al., 2001), and may also bind an SH3 domain of Nck1 by a similar mechanism (Barda-Saad et al., 2010). In addition, Vav1 associates with the Itk kinase, though the Vav1 domains required for this are unknown (Bunnell et al., 2000; Dombroski et al., 2005).

The recruitment of TCR proximal signalling molecules to microclusters at the IS, and the documented association of Vav1 with some of these, has led to the expectation that Vav1 may also move to the IS. Biochemical and imaging studies in the Jurkat T cell leukaemic cell line and in mouse CD4<sup>+</sup> T cells have shown that Vav1 is located in the cytoplasm in resting cells, but recruited to the plasma membrane following TCR stimulation and to the IS in T cell:APC conjugates (Groysman et al., 2002; Miletic et al., 2006; Singleton et al., 2011; Sylvain et al., 2011; Tamir et al., 2000; Villalba et al., 2001; Xavier et al., 1998; Zeng et al., 2003; Zhang et al., 1998). However no studies to date have examined the localisation of Vav1 in CD8<sup>+</sup> T cells. In this study, using primary CD4<sup>+</sup> and CD8<sup>+</sup> T cells, we show that Vav1 redistributes to the IS in conjugates and to microclusters following TCR stimulation, we identify that the SH2 and SH3<sub>B</sub> domains of Vav1 are required for this movement, and show that the recruitment depends on Y112 and Y128 of SLP76. Furthermore, we show that the SH2 and SH3<sub>B</sub> domains of Vav1 are also required for its phosphorylation and subsequent activation of GEF activity, and for TCR-induced calcium flux, thereby demonstrating that both the GEF-dependent and -independent signalling functions of Vav1 require its correct localisation.

### Fig. 1. Localisation of Vav1 in primary CD4<sup>+</sup> and CD8<sup>+</sup> T cells.

(A,B,C) Activated CD4<sup>+</sup> DO11.10 T cells conjugated with APCs (B cells from BALB/c-*Vav1*<sup>-/-</sup> mice) loaded or not with the OVA peptide. (D,E,F) Activated CD8<sup>+</sup> F5 T cells conjugated with APCs (B cells from 129S8-*Vav1*<sup>-/-</sup> mice) loaded or not with the NP68 peptide. (A,D) Images show single optical sections of T cell:APC conjugates stained with antibodies against phosphotyrosine (pY) and Vav1, as well as DIC images. APCs are indicated with asterisks. Scale bar: 10  $\mu$ m. (B,E) Recruitment index (mean  $\pm$  SEM) of pY and Vav1 in the T cells, a measure of polarisation towards the IS, quantified from images such as those shown in (A) and (D), either in conjugates generated in the absence of cognate peptide, or after 5–40 min of conjugate formation, as indicated. *n* indicates the number of cells scored for each time point. (C) and (F) Percentage of T cells showing accumulation of pY and Vav1 towards the IS. (G) CD4<sup>+</sup> DO11.10 or CD8<sup>+</sup> F5 T cells expressing EGFPVav1 were conjugated for 7 min with OVA peptide-pulsed or NP68-pulsed APCs (B cells from *Vav1*<sup>-/-</sup> mice). Images show single optical sections of T cell:APC conjugates stained with antibodies against EGFP and phosphotyrosine (pY), as well as phase images. APCs are indicated with asterisks. Scale bar: 5  $\mu$ m. (H,I) (H) 5C.C7 CD4<sup>+</sup> T cells expressing EGFPVav1 were conjugated with CH27 cells pulsed with MCC peptide or (I) P14 CD8<sup>+</sup> T cells expressing EGFP-Vav1 were conjugated with B cells pulsed with gp33 peptide. The graphs display the percentage of cell couples that displayed accumulation of EGFPVav1 with the indicated patterns as a function of time relative to formation of tight cell couples (Singleton et al., 2009). Statistically significant differences were determined with a *t*-test; \**P*<0.05, \*\**P*<0.01, \*\*\**P*<0.001.

## Results

### Vav1 is recruited to the immunological synapse in both CD4<sup>+</sup> and CD8<sup>+</sup> primary T cells

To investigate the recruitment of Vav1 to the synapse in primary CD4<sup>+</sup> T cells we used DO11.10 TCR transgenic T cells, which are specific for an ovalbumin peptide (OVA323-339) presented on I-A<sup>d</sup> (Murphy et al., 1990). Activated DO11.10 T cells were mixed with primary B cells from Vav1-deficient mice as antigen-presenting cells (APCs) that had been pulsed with OVA peptide to induce formation of T cell:APC conjugates. We used Vav1-deficient APCs so that an anti-Vav1 antibody would detect Vav1 only in T cells. Cells were fixed at different time points and stained with antibodies against phosphotyrosine (a mark of active signalling) and against Vav1, and imaged by confocal microscopy. Analysis showed clear accumulation of both phosphotyrosine and Vav1 at the immunological synapse (IS) between the T cells and the APCs (Fig. 1A–C). Similarly, we analysed recruitment of Vav1 to the IS in CD8<sup>+</sup> T cells using F5 TCR transgenic T cells, which are specific for the NP68 peptide presented on H-2D<sup>b</sup> (Mamalaki et al., 1993). Once again, activated F5 T cells were mixed with primary B cells from Vav1-deficient mice as APCs that had been pulsed with NP68

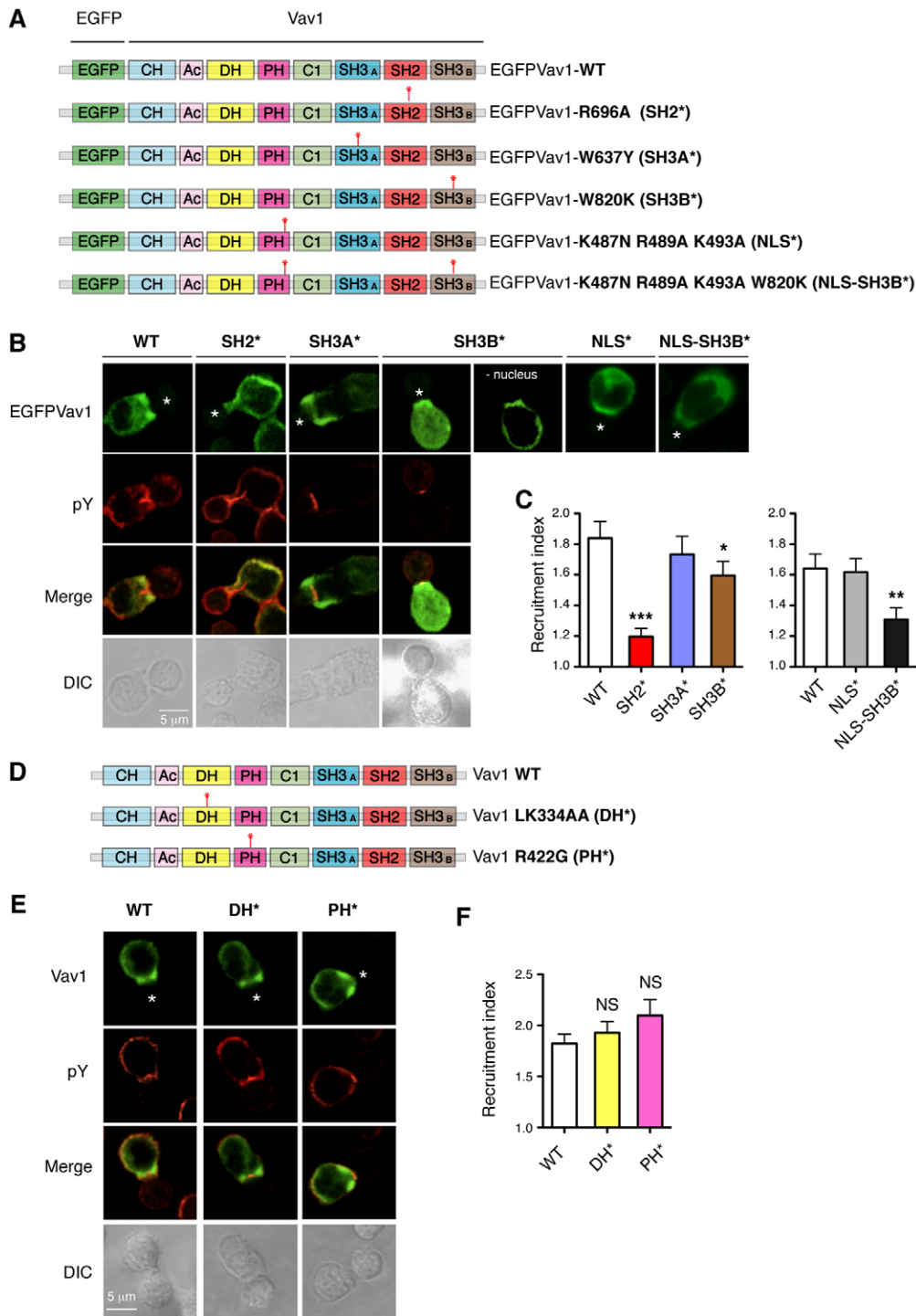


**Fig. 2. Correct localisation of mutant Vav1 proteins in F5 CD8<sup>+</sup> T cells requires the SH2 and SH3<sub>B</sub> domains.** (A) Schematic representation of EGFPVav1 constructs used in this study. The mutations in the SH2 (R696A), SH3<sub>A</sub> (W637Y), and SH3<sub>B</sub> (W820K) domains of Vav1 and a mutation disabling the putative nuclear localisation signal (NLS) (K487N R489A K493A) are highlighted with asterisks. (B) CD8<sup>+</sup> F5 T cells expressing EGFPVav1 wild-type (WT), SH2, SH3<sub>A</sub>, SH3<sub>B</sub>, NLS and NLS-SH3B mutants were conjugated for 7 min with NP68-pulsed APCs (B cells from 129S8-*Vav1*<sup>-/-</sup> mice). Images show single optical sections of T cell:APC conjugates stained with antibodies against phosphotyrosine (pY) and EGFP, as well as DIC images. APCs are indicated with asterisks. For quantification of the SH3<sub>B</sub> mutant, the EGFP signal from the nucleus was digitally subtracted as shown. Scale bar: 5 μm. (C) Graphs showing mean (±SEM) recruitment index of EGFPVav1 quantitated from images such as those shown in (B). Number of cells analysed (n): WT (75), SH2\* (103), SH3A\* (76), SH3B\* (63), NLS\* (74), NLS-SH3B\* (66). Statistically significant differences were determined with a *t*-test; \**P*<0.05, \*\**P*<0.01, \*\*\**P*<0.001. (D) Schematic representation of Vav1 proteins with mutations in the DH (LK334AA) and PH (R422G) domains as highlighted with asterisks. (E) CD8<sup>+</sup> F5 T cells expressing WT Vav1 or Vav1 with mutations in the DH or PH domains were conjugated for 7 min with NP68-pulsed APCs (B cells from 129S8-*Vav1*<sup>-/-</sup> mice). Images show single optical sections of T cell:APC conjugates stained with antibodies against phosphotyrosine (pY) and Vav1, as well as DIC images. APCs are indicated with asterisks. Scale bar: 5 μm. (F) Graphs showing mean (±SEM) recruitment index of Vav1 quantitated from images such as those shown in (E). Number of cells analysed (n): WT (102); DH\* (71); PH\* (70). The recruitment index in the DH and PH mutants was not significantly (NS) different to wild-type Vav1.

peptide to induce formation of T cell:APC conjugates. Image analysis of conjugates stained with antibodies against both phosphotyrosine and Vav1 showed that both accumulated at the IS (Fig. 1D–F). Thus Vav1 is recruited to the IS in both CD4<sup>+</sup> and CD8<sup>+</sup> primary T cells.

To allow further analysis of the mechanism of recruitment of Vav1 to the IS, we generated a retroviral vector expressing a fusion protein between enhanced green fluorescent protein (EGFP) and Vav1 (EGFP-Vav1). Imaging of DO11.10 CD4<sup>+</sup> and F5 CD8<sup>+</sup> T cells infected with this viral vector showed that similar to Vav1, EGFP-Vav1 was also recruited to the IS of primary CD4<sup>+</sup> and CD8<sup>+</sup> T cells in peptide specific-conjugates with APCs, but not in the absence of peptide (Fig. 1G, and data not shown). Initially we used this fusion protein to image the movement of Vav1 to the IS in real time, and to classify the pattern of recruitment in terms of the distribution of Vav1 at the IS (Singleton et al., 2009). The EGFP-Vav1 expressing retroviral vector was used to infect 5C.C7 CD4<sup>+</sup> or P14 CD8<sup>+</sup> T cells and these were conjugated with APCs pulsed with agonist peptides. Image analysis of the conjugates was used to define the distribution of EGFP-Vav1 at the IS as a function of time. This showed that peak recruitment of EGFP-Vav1 occurred in the first 2 min following conjugate formation and that most of the EGFP-Vav1 had a peripheral, diffuse or lamellar distribution across the IS (Fig. 1H,I). EGFP-Vav1 was not found concentrated at the centre of the IS in either CD4<sup>+</sup> or CD8<sup>+</sup> T cells. While the distribution of Vav1 was broadly similar between CD4<sup>+</sup> and CD8<sup>+</sup> T cells, the kinetics were somewhat different, with Vav1 persisting for longer at the IS in CD4<sup>+</sup> T cells compared to CD8<sup>+</sup> T cells (Fig. 1B,C,E,F,H,I). This may reflect functional differences between the cell types; in particular, the cytotoxic responses of CD8<sup>+</sup> T cells occur very rapidly, within 4–5 min of conjugate formation (Stinchcombe et al., 2001). We also note that while phosphotyrosine was usually found in the peripheral regions of the IS in CD4<sup>+</sup> T cells, it was generally most abundant centrally in CD8<sup>+</sup> T cells, in agreement with previous reports of

active signalling in the cSMAC of CD8<sup>+</sup> T cells (Fig. 1A,D) (Beal et al., 2009; Jenkins et al., 2009; O'Keefe et al., 2004; Stinchcombe et al., 2001).

### The SH2 and SH3<sub>B</sub> domains of Vav1 are required for recruitment to the immunological synapse

Next we used the EGFP-Vav1 protein to determine which domains of Vav1 were required for recruitment to the IS. We generated retroviral vectors expressing EGFP-Vav1 with point mutations in the SH2, SH3<sub>A</sub> and SH3<sub>B</sub> domains (Fig. 2A). The R696A mutation (SH2\*) abolishes the ability of the SH2 domain of Vav1 to bind phosphotyrosine containing peptides; the W637Y mutation (SH3A\*) abolishes binding of the SH3<sub>A</sub> domain of Vav1 to the C-terminal SH3 domain of Grb2 (Nishida et al., 2001); the W820K mutation (SH3B\*) abolishes the ability of the SH3<sub>B</sub> domain of Vav1 to bind poly-proline motifs in target proteins. Expression of these mutant EGFP-Vav1 proteins in CD8<sup>+</sup> F5 T cells showed that mutation of the SH2 domain strongly reduced recruitment of the protein to the IS (Fig. 2B,C). Mutation of the SH3<sub>B</sub> domain also decreased recruitment, but the effect was only partial. In contrast the SH3<sub>A</sub> mutation had no effect on recruitment to the IS. The SH2 domain of EGFP-Vav1 was also required for recruitment to the IS of CD4<sup>+</sup> primary T cells as shown by imaging of conjugates between DO11.10 or 5C.C7 T cells and agonist peptide-pulsed APCs (Fig. 3A–D).

In imaging the SH3B\* mutant EGFP-Vav1, we noticed that much of the protein was in the nucleus, in contrast to wild-type Vav1 (Fig. 2B). Earlier studies had shown that deletion of the SH3<sub>B</sub> domain of Vav1 caused the protein to move into the nucleus (Houliard et al., 2002). In this work, the authors had defined a nuclear localisation signal (NLS) in the PH domain of Vav1. We wondered if the reduced recruitment of EGFP-Vav1-SH3B\* to the IS might be due to localisation of some of the protein to the nucleus, rather than a direct role for the SH3<sub>B</sub> domain in IS recruitment. To address this, we designed a novel mutation to inactivate the NLS. Previous work had deleted eight

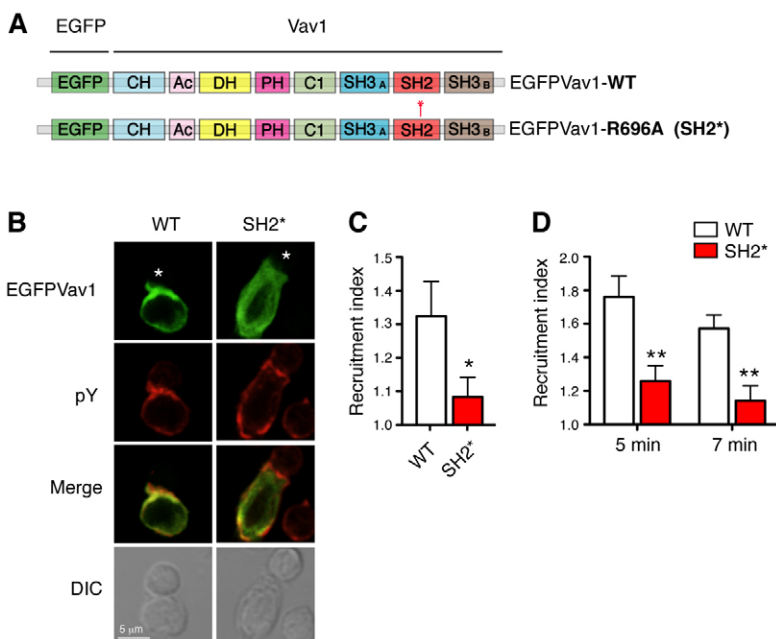


**Fig. 3. The SH2 domain of Vav1 is required for correct localisation in CD4<sup>+</sup> T cells.** (A) Schematic representation of EGFPVav1 WT and SH2 mutant constructs used in this study. The SH2 mutation is highlighted with an asterisk. (B) CD4<sup>+</sup> DO11.10 T cells expressing WT Vav1 or Vav1 with a mutation in the SH2 domain were conjugated for 7 min with OVA peptide-pulsed APCs (B cells from BALB/c-*Vav1*<sup>-/-</sup> mice). Images show single optical sections of T cell:APC conjugates stained with antibodies against phosphotyrosine (pY) and EGFP, as well as DIC images. APCs are indicated with asterisks. Scale bar, 5 μm. (C) Graph showing mean (±SEM) recruitment index of EGFPVav1 quantitated from images such as those shown in (B). Number of cells analysed: WT (50), SH2\* (57). (D) Graph showing mean (±SEM) recruitment index of EGFPVav1 in 5C.C7 CD4<sup>+</sup> T cells conjugated with CH27 B cell lymphoma APCs pulsed with 10 μM MCC agonist peptide, and imaged 5 and 7 min after initiation of conjugate formation. Number of cell analysed: WT (14), SH2\* (11 at 5 min, 7 at 7 min). Statistically significant differences were determined with a *t*-test; \**P* < 0.05, \*\**P* < 0.01.

amino acids in the NLS; however, several of these residues play a structural role in the PH domain of Vav1, and thus the mutation could result in unfolding of the domain, with unpredictable consequences (Houlard et al., 2002; Rapley et al., 2008). In contrast, we mutated just three amino acids (K487N, R489A, K493A), which are the only basic residues in the NLS that play no obvious structural role. When combined with the SH3B\* mutation, this novel NLS mutation (NLS\*) abolished localisation of EGFP-Vav1-SH3B\* to the nucleus (Fig. 2A,B), thus allowing study of the SH3B\* mutation in the absence of confounding

effects from nuclear localisation. Image analysis of mutant EGFP-Vav1 proteins in F5 T cell conjugates showed that the NLS\* mutation on its own had no effect on EGFP-Vav1 recruitment to the IS, whereas the double mutant still showed reduced recruitment (Fig. 2B,C). Thus we conclude that the SH3<sub>B</sub> domain of Vav1 is required for normal IS recruitment.

To analyse a potential role for the DH and PH domains of Vav1 in recruitment to the IS, we made use of mice bearing point mutations in these domains (Fig. 2D). The L334A K335A (LK334AA, DH\*) mutation abolishes the GEF activity of Vav1

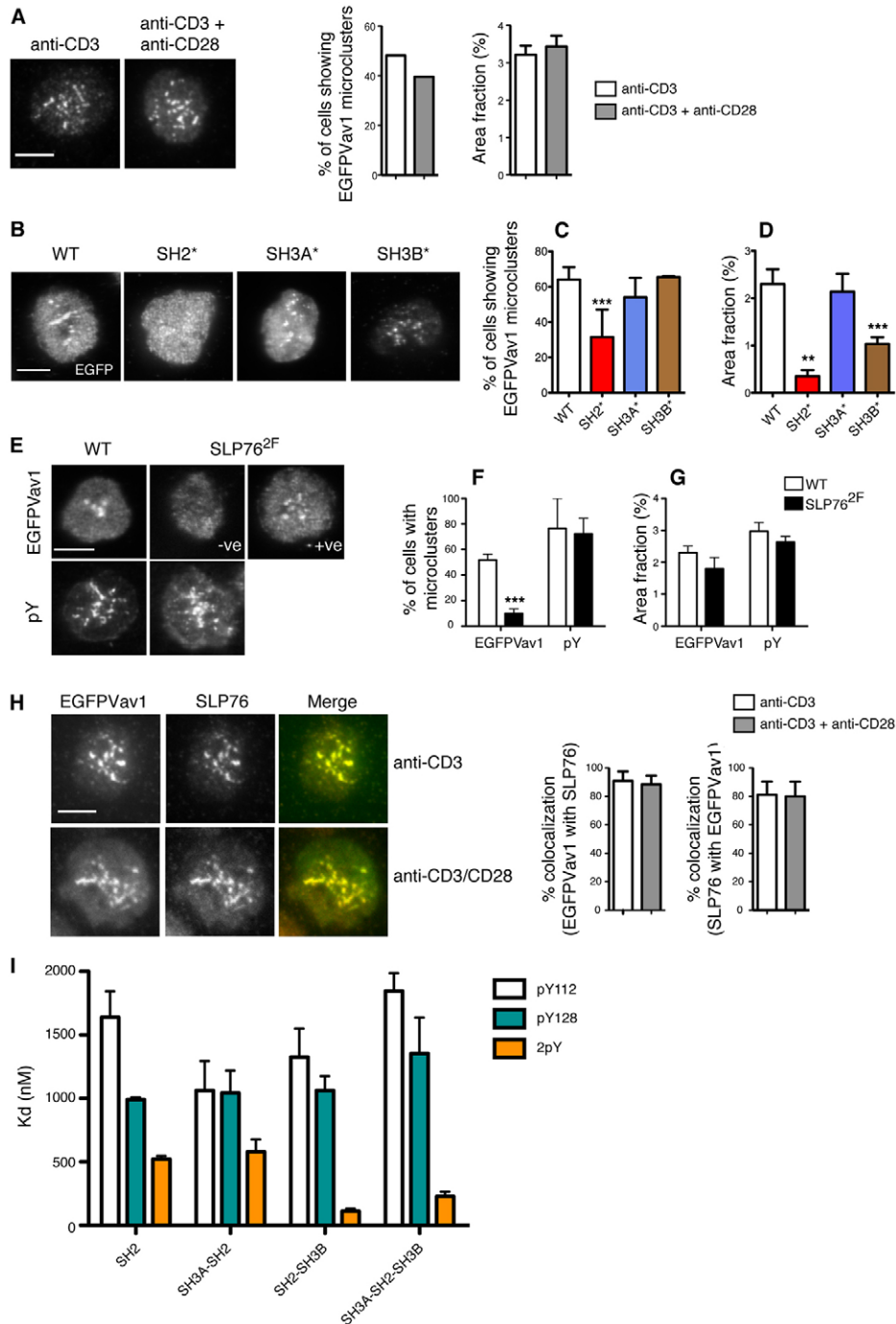


Fig. 4. See next page for legend.

without perturbing folding of the DH domain (Saveliev et al., 2009); the R422G mutation (PH\*) abolishes binding of phosphoinositides to the PH domain (Han et al., 1998; Prisco et al., 2005). Image analysis of F5 CD8<sup>+</sup> T cells expressing the DH\* or PH\* mutant Vav1 in conjugates with APCs showed that neither mutation affected recruitment of Vav1 to the IS (Fig. 2E,F). Taken together we conclude that the SH2 and SH3<sub>B</sub> domains of Vav1 are required for normal recruitment to the IS in primary T cells, whereas the DH, PH and SH3<sub>A</sub> domains show no critical role in this process.

### The SH2 and SH3<sub>B</sub> domains of Vav1 are required for recruitment to microclusters

Next we examined whether Vav1 is recruited to microclusters at the IS by using total internal reflection fluorescence microscopy (TIRFM) to image EGFP-Vav1 in CD4<sup>+</sup> T cells plated for 3 minutes onto coverslips coated with stimulatory antibodies. Previous studies had shown the induction of TCR microclusters in Jurkat T cells plated onto anti-CD3ε or in primary T cells plated onto anti-CD3ε and anti-CD28 antibodies (Barda-Saad

et al., 2005; Braiman et al., 2006; Bunnell et al., 2002). Since Vav1 is phosphorylated in response to stimulation through both the TCR and CD28 and both TCR and CD28 transduce signals via Vav1 (Michel et al., 2000; Nunes et al., 1996; Raab et al., 2001; Tybulewicz, 2005), we compared T cells interacting with anti-CD3ε in the presence or absence of anti-CD28 antibodies. We found that EGFP-Vav1 is rapidly recruited to microclusters in cells plated onto anti-CD3ε, and the frequency of cells with Vav1 microclusters, or the size of the clusters was not changed by inclusion of anti-CD28 (Fig. 4A; supplementary material Movies 1, 2).

Examination of T cells expressing mutant forms of EGFP-Vav1 showed that the SH2\* mutant strongly decreased recruitment into microclusters as measured by the percentage of cells showing microclusters of EGFP-Vav1 and the fractional area occupied by EGFP-Vav1 microclusters (Fig. 4B–D). The SH3B\* mutation also affected recruitment into microclusters, however the effect was partial as it resulted in decreased fractional area occupied by EGFP-Vav1 microclusters, but had no effect on the percentage of cells showing microclusters (Fig. 4B–D). In contrast, the SH3A\* mutation had no effect on recruitment of EGFP-Vav1 to microclusters (Fig. 4B–D). Thus, as with recruitment to the IS in general, the specific recruitment of Vav1 to microclusters also requires the SH2 and, to a lesser extent, the SH3<sub>B</sub> domains.

### The recruitment of Vav1 to microclusters depends on Y112 and Y128 of SLP76

The SH2 domain of Vav1 has been previously reported to bind phosphotyrosine (pY) 112 and pY128 of the SLP76 adaptor protein. To examine whether the recruitment of Vav1 to microclusters at the IS is dependent on the phosphorylation of these two residues we made use of T cells from SLP76<sup>2F</sup> mice carrying mutations in SLP76 where both tyrosine residues had been replaced with phenylalanines (Y112F, Y128F) (Jordan et al., 2008). SLP76<sup>2F</sup> CD4<sup>+</sup> T cells were infected with a retrovirus expressing EGFP-Vav1 and the recruitment of the fusion protein was monitored by TIRFM. Analysis showed that while the SLP76<sup>2F</sup> mutation did not affect the formation of microclusters as judged by staining for phosphotyrosine, it caused a large reduction in the recruitment of Vav1 (Fig. 4E–G). If Vav1 is recruited to microclusters via binding to SLP76, the distributions of the two proteins should be similar. Indeed TIRFM analysis showed a very high degree of co-localisation of EGFP-Vav1 and SLP76 in cells plated onto either anti-CD3ε alone or anti-CD3ε with anti-CD28 (Fig. 4H, Pearson's correlation coefficient,  $r=0.959\pm 0.002$  or  $0.960\pm 0.003$ , respectively).

Previous studies had shown that mutation of either Y112 or Y128 of SLP76 abolished the interaction of the adaptor protein with Vav1 (Fang and Koretzky, 1999). Given that the sequences surrounding Y112 and Y128 of SLP76 are very similar and both fit the consensus binding site for the Vav1 SH2 domain (Songyang et al., 1994), it is not clear why mutation of either residue alone would lead to loss of Vav1-SLP76 association. One possible explanation is that there is co-operative binding between two Vav1 molecules each binding to one pY on SLP76. To explore this binding further we expressed the SH2 domain of Vav1 in *E.coli*, purified it and used isothermal titration calorimetry (ITC) to assess its ability to bind to peptides from SLP76 containing pY112, pY128 or both residues (2pY). We found that the SH2 domain bound to peptides containing either

**Fig. 4. Recruitment of Vav1 into microclusters requires the SH2 and SH3<sub>B</sub> domains of Vav1 and Y112 and Y128 of SLP76.** (A) TIRFM images of EGFP in CD4<sup>+</sup> T cells expressing EGFPVav1. Cells were activated for 3 min on coverslips coated with anti-CD3ε ± anti-CD28 antibodies and stained for GFP. Scale bar: 5 μm. Graphs show mean (±SEM) percentage of CD4<sup>+</sup> T cells forming EGFPVav1 microclusters and mean (±SEM) area fraction occupied by microclusters (area of clusters/cell area), calculated only in cells that formed any microclusters; inclusion of anti-CD28 caused no significant change in either of these parameters. (B) TIRFM images of EGFP in CD4<sup>+</sup> T cells expressing EGFPVav1-WT, SH2, SH3<sub>A</sub> or SH3<sub>B</sub> domain mutants. Cells were activated for 3 min on coverslips coated with anti-CD3ε and anti-CD28 antibodies and stained for GFP. Scale bar: 5 μm. (C) Mean (±SEM) percentage of CD4<sup>+</sup> T cells forming EGFPVav1 microclusters. Data are from two independent experiments. Number of cells analysed (n): EGFPVav1-WT (72), EGFPVav1-SH2\* (43), EGFPVav1-SH3A\* (73), EGFPVav1-SH3B\* (100). Statistically significant differences were determined with Fisher's exact test; \*\*\* $P<0.001$ . (D) Mean (±SEM) area fraction occupied by microclusters, calculated only in cells that formed any microclusters. Number of cells analysed (n): EGFPVav1-WT (46), EGFPVav1-SH2\* (13), EGFPVav1-SH3A\* (33), EGFPVav1-SH3B\* (66). Statistically significant differences were determined with a *t*-test; \*\* $P<0.01$ , \*\*\* $P<0.0001$ . (E) TIRFM images of WT or SLP76<sup>2F</sup> CD4<sup>+</sup> T cells expressing wild-type EGFPVav1. Cells were activated for 3 min on anti-CD3ε and anti-CD28 coated coverslips and stained for GFP or phosphotyrosine (pY). Scale bar: 5 μm. For SLP76<sup>2F</sup> T cells, example images are shown of cells without (–ve) and with (+ve) EGFPVav1 microclusters. (F) Mean percentage of CD4<sup>+</sup> T cells (WT or SLP76<sup>2F</sup>) forming EGFPVav1 or phosphotyrosine microclusters. Data are from five (EGFPVav1) and two (pY) independent experiments. Number of cells analysed (n): WT T cells - EGFPVav1 (163), pY (67); SLP76<sup>2F</sup> T cells - EGFPVav1 (169), pY (123). Statistically significant differences were determined with Fisher's exact test; \*\*\* $P<0.001$ . (G) Mean (±SEM) area fraction occupied by microclusters, calculated only in cells that formed any microclusters. Number of cells analysed (n): WT T cells - EGFPVav1 (80), pY (39); SLP76<sup>2F</sup> T cells - EGFPVav1 (15), pY (84). (H) TIRFM images of CD4<sup>+</sup> T cells activated for 3 min on coverslips coated with anti-CD3ε ± anti-CD28 antibodies and stained for GFP or SLP76. The merged images show an overlay of EGFPVav1 (green) and SLP76 (red) with colocalization visualised by a yellow colour. Scale bar, 5 μm. Graphs show the mean (±SD) percentage colocalization of EGFPVav1 with SLP76 and vice-versa. (I) Graph shows mean (±SEM) dissociation constants ( $K_d$ ) of binding between the indicated Vav1 fragments and peptides from SLP76 (pY112, pY128 and 2pY) determined by isothermal titration calorimetry.

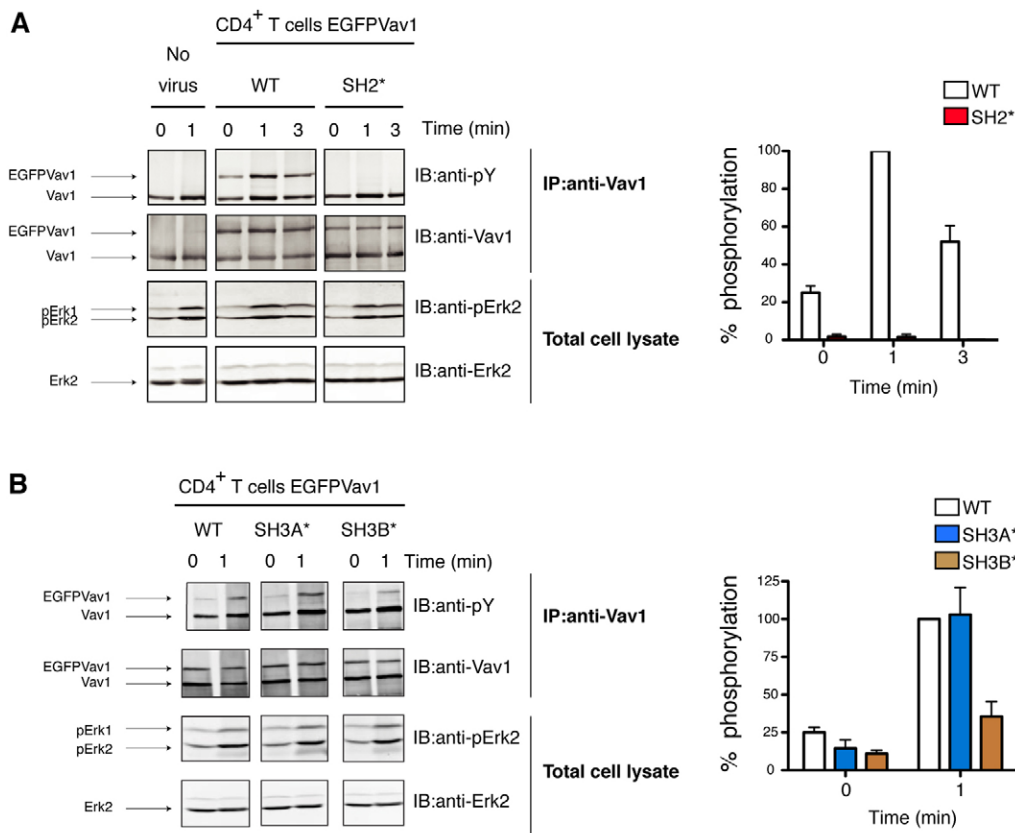
pY112 or pY128 with a dissociation constant ( $K_d$ ) of 1640 nM and 990 nM, respectively (Fig. 4I). The binding of the SH2 domain to a peptide containing both pY112 and pY128 showed a  $K_d$  of 520 nM and a stoichiometry of 2:1 (SH2 domain:peptide), implying that each pY could independently bind the Vav1 SH2 domain, with a small enhancement of affinity in the two pY peptide compared to the single pY peptides (Fig. 4I, and data not shown). There was no detectable binding to a peptide in which both Y112 and Y128 were unphosphorylated (not shown).

Next we examined the ability of a 3-domain SH3<sub>A</sub>-SH2-SH3<sub>B</sub> fragment of Vav1 to bind to these peptides. Again binding to the single pY peptides occurred with  $K_d$ s in the micromolar range (1846 nM and 1353 nM for the pY112 and pY128 peptides respectively; Fig. 4I). However binding to the 2pY peptide was significantly stronger with a  $K_d$  of 227 nM, and a stoichiometry of two SH3<sub>A</sub>-SH2-SH3<sub>B</sub> molecules binding to one peptide (Fig. 4I, and data not shown). Again there was no detectable binding to an unphosphorylated peptide (not shown). This enhancement in affinity when using the 3-domain fragment of Vav1 and the 2pY peptide suggests that there is co-operativity of binding, perhaps as a result of additional interactions between the two Vav1 fragments, or between Vav1 and the peptide, outside the SH2-pY binding pocket, although the latter is unlikely as we saw no measurable binding with the unphosphorylated peptide. To identify whether the SH3<sub>A</sub> or SH3<sub>B</sub> domains contributed to this enhanced binding, we measured the affinities of SH3<sub>A</sub>-SH2 and SH2-SH3<sub>B</sub> 2-domain fragments for the pY peptides. The SH3<sub>A</sub>-SH2 fragment behaved like the isolated SH2 domain with weaker affinity for the single pY peptides ( $K_d$ : 1062 nM and 1043 nM for pY112 and pY128, respectively) and slightly

enhanced binding to the 2pY peptide ( $K_d$ : 579 nM) (Fig. 4I). By contrast, the SH2-SH3<sub>B</sub> fragment behaved similarly to the 3-domain fragment with weaker binding to the single pY peptides ( $K_d$ : 1325 nM and 1062 nM for pY112 and pY128, respectively), but strongly enhanced binding to 2pY ( $K_d$ : 111 nM) (Fig. 4I). Once again the stoichiometry of the interaction was 2 Vav1 fragments to one 2pY peptide (not shown). These results show that the SH2 domain of Vav1 binds to both pY112 and pY128 of SLP76, and that the binding of two Vav1 molecules to the 2pY peptide of SLP76 is enhanced by the presence of the SH3<sub>B</sub> domain.

### The SH2 and SH3<sub>B</sub> domains of Vav1 are required for its phosphorylation

Next we examined the functional consequences of recruitment of Vav1 to microclusters at the IS. Vav1 is phosphorylated on tyrosine residues following TCR stimulation, a process required for full activation of its GEF activity (Tybulewicz, 2005). To evaluate the effects of domain mutations on phosphorylation of Vav1, we used retroviral infection to express wild-type and mutant EGFP-Vav1 in primary CD4<sup>+</sup> T cells, and then examined TCR-induced phosphorylation of the fusion protein. We found that the SH2\* mutation caused a complete loss of tyrosine phosphorylation of EGFP-Vav1 (Fig. 5A). In contrast, mutation of the SH3A domain had no effect, whereas the SH3B\* mutation caused a partial reduction in phosphorylation (Fig. 5B). In previous studies we had shown that the PH\* and DH\* mutations did not affect tyrosine phosphorylation of Vav1, suggesting that the function of these domains is not critical for this process (Prisco et al., 2005; Saveliev et al., 2009). Thus the same



mutations in the SH2 and SH3<sub>B</sub> domains that, respectively, completely or partially reduce recruitment to the IS and to microclusters, also cause complete or partial loss of phosphorylation, suggesting that recruitment of Vav1 to the IS through these domains is required for phosphorylation, and hence for activation of GEF activity.

### The SH2 and SH3<sub>B</sub> domains of Vav1 are required for TCR-induced calcium flux

In addition to its GEF-dependent functions, Vav1 also has GEF-independent functions transducing TCR signals to calcium flux. Previous studies had indicated that Vav1 is required for TCR-induced activation of PLC $\gamma$ 1 and hence to the production of inositol-3,4,5-trisphosphate (IP<sub>3</sub>), a second messenger that triggers release of Ca<sup>2+</sup> from intracellular stores (Reynolds et al., 2002). As expected from these earlier observations, Vav1-deficient CD4<sup>+</sup> and CD8<sup>+</sup> T cells show a defective TCR-induced calcium flux, when cells were stimulated in the presence of EGTA to chelate extracellular calcium and thus limit the calcium flux to release from intracellular stores (Fig. 6A).

To evaluate whether mutations in the SH2 or SH3 domains perturb this function of Vav1, we used retroviral infection to express wild-type or mutant EGFP-Vav1 proteins in Vav1-

deficient CD4<sup>+</sup> T cells. Once again we found that mutation of the SH3<sub>A</sub> domain had no effect, mutation of the SH3<sub>B</sub> domain partially reduced TCR-induced calcium flux, whereas the SH2\* mutation resulted in no increase in calcium flux above that seen in Vav1-deficient T cells (Fig. 6B,C). To understand whether the reduced calcium flux in T cells expressing the SH3B\* mutant was due to its partial nuclear localisation, or to a cytoplasmic function for this domain, we also compared the TCR-induced calcium flux in Vav1-deficient T cells expressing the NLS\* and NLS\*-SH3B\* mutant EGFP-Vav1. These studies show that the NLS\* mutation does not affect TCR-induced calcium flux, whereas the NLS\*-SH3B\* mutant is once again partially compromised (Fig. 6C). In conclusion, as with recruitment to the IS and with TCR-induced phosphorylation, the SH2 domain is critical for the ability of Vav1 to transduce TCR signals to the rise in intracellular calcium, while the SH3<sub>B</sub> domain plays a more minor, yet detectable, role.

### Discussion

We have shown that, in common with many other signalling molecules that transduce proximal TCR signals, Vav1 is recruited to the IS of primary CD4<sup>+</sup> and CD8<sup>+</sup> T cells. Dynamic imaging of both 5C.C7 CD4<sup>+</sup> and P14 CD8<sup>+</sup> T cells showed that Vav1 was

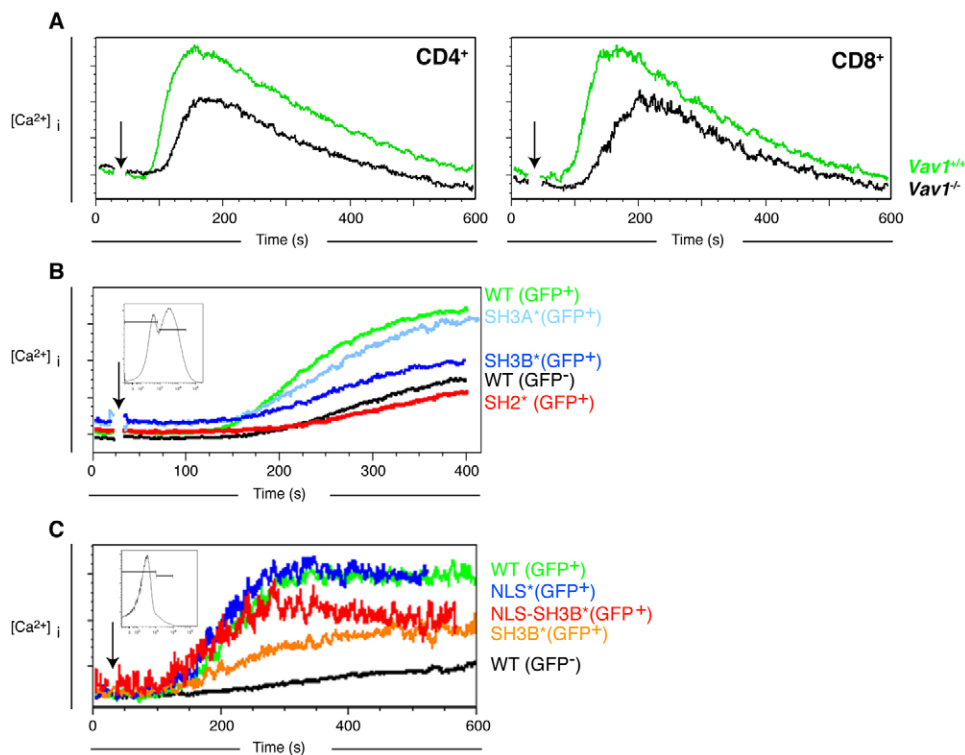


**Fig. 6. The SH2 and SH3<sub>B</sub> domains of Vav1 are required for normal TCR-induced calcium flux.** (A) Graphs show mean ratio of Indo-1 violet/blue fluorescence, a measure of intracellular Ca<sup>2+</sup> as a function of time in Vav1<sup>+/+</sup> (green) or Vav1<sup>-/-</sup> (black) CD4<sup>+</sup> or CD8<sup>+</sup> T cells in the presence of EGTA to chelate extracellular calcium, thus limiting calcium flux to release from intracellular stores. The time at which cells were stimulated with crosslinking antibody is indicated by a vertical arrow. (B,C) Vav1-deficient CD4<sup>+</sup> T cells were transduced with (B) retroviruses expressing EGFPVav1 WT or SH2\*, SH3A\* and SH3B\* mutants, or with (C) retroviruses expressing EGFP-WT, or NLS\*, SH3B\* and NLS-SH3B\* mutants. Inset histograms show EGFP expression in T cells transduced with retroviruses expressing EGFPVav1 WT protein, and markers show gates used to distinguish GFP<sup>+</sup> and GFP<sup>-</sup> cells. Graphs show mean ratio of Indo-1 violet/blue fluorescence, a measure of intracellular Ca<sup>2+</sup> as a function of time in Vav1-deficient CD4<sup>+</sup> T cells expressing indicated constructs and gated as on histograms. To demonstrate the calcium flux in Vav1-deficient T cells, GFP<sup>-</sup> cells are shown from cultures infected with a virus expressing EGFP Vav1 WT. In all other cases, only GFP<sup>+</sup> cells are shown. The time at which cells were stimulated with crosslinking antibody is indicated by a vertical arrow. One representative experiment out of three is shown.

localised predominantly to the periphery of the IS or diffusely across the cell-cell interface, corresponding most closely to the pSMAC distribution. A similar distribution was also seen in DO11.10 CD4<sup>+</sup> T cells where the distribution of Vav1 was most closely correlated to that of F-actin and active Cdc42 (Singleton et al., 2011). Furthermore, in CD4<sup>+</sup> T cells Vav1 was found in microclusters at the plasma membrane following stimulation with immobilised anti-CD3 $\epsilon$  in the presence or absence of anti-CD28 antibodies. This recruitment to the IS and to microclusters was completely dependent on the SH2 domain of Vav1 and partially dependent on a functional SH3<sub>B</sub> domain. In contrast we found no requirement for the DH, PH or SH3<sub>A</sub> domains. Furthermore, we showed that Vav1 recruitment to microclusters was dependent on Y112 and Y128 of SLP76, suggesting that this may be due to direct binding of the Vav1 SH2 domain to these residues once they become phosphorylated. Such an interpretation was supported by a high degree of co-localisation of Vav1 and SLP76 in microclusters. In addition, biophysical studies showed that the SH2 domain of Vav1 binds to both pY112 and pY128, that a doubly phosphorylated peptide can recruit two Vav1 SH2 domains, and that this binding was strongly enhanced by the presence of the SH3<sub>B</sub> domain. This cooperative binding of two Vav1 molecules to one SLP76 molecule potentially explains why both the SH2 and SH3<sub>B</sub> domains of Vav1 are required for recruitment to the IS and to microclusters, and may also explain the observation that mutation of either Y112 or Y128 causes loss of Vav1-SLP76 association, despite the ability of the Vav1 SH2 domain to bind to either phosphotyrosine (Fang and Koretzky, 1999).

In some PH domain-containing proteins the PH domain binds phosphoinositides and this interaction is required for membrane recruitment (Lemmon, 2008). The PH domain of Vav1 also binds phosphoinositides (Han et al., 1998), however our data show that this binding is not required for recruitment to the IS. Our results agree with a recent study in Jurkat T cells, which showed that the SH2 domain of Vav1 is required for its recruitment to SLP76-containing microclusters and that mutation of the SH3<sub>B</sub> domain partially inhibits this movement (Sylvain et al., 2011). In contrast to our results, the same study also found a partial role for the SH3<sub>A</sub> domain in this recruitment. The reason for this discrepancy is unknown, but may be due to differences between Jurkat cells and primary mouse T cells, or to the use of a different mutation (P657A), though we note that both this mutation and the one we have used (W637Y) are predicted to abolish binding to the SH3 domain of Grb2 (Nishida et al., 2001). In another study in Jurkat cells, the binding of Vav1 to SLP76 was abrogated by mutations in Y112 and Y128 of SLP76, in agreement with our data in primary T cells (Barda-Saad et al., 2010). However the same study showed that in Jurkat cells association of Vav1 with SLP76 was dependent on the adaptor protein Nck. The authors proposed that through its SH2 domain, Nck binds to pY112 and pY128 on SLP76, and through its C-terminal SH3 domain binds to the SH3<sub>A</sub> domain of Vav1, thereby bridging the binding of SLP76 and Vav1. Such a model predicts that the SH3<sub>A</sub> domain of Vav1 is important for its recruitment, but provides no role for the SH2 domain in this process, in contrast to our results. It is certainly possible that a Vav1-Nck-SLP76 complex is formed in T cells, stabilised by multiple domain interactions, however the lack of any effect of the SH3<sub>A</sub> mutation on Vav1 recruitment suggests that in primary mouse T cells the Vav1-Nck interaction may be less critical for the movement of Vav1.

Our studies showed that mutation of a single amino acid in the SH3<sub>B</sub> domain (W820K) causes a large fraction of Vav1 to localise to the nucleus. This is similar to results in a previous study showing that deletion of SH3<sub>B</sub> causes Vav1 to move to the nucleus of RBL-2H3 cells, a mast cell line (Houlard et al., 2002). In this study the authors had defined an eight amino acid NLS located within the PH domain that was required for nuclear localisation. Inspection of the structure of Vav1 showed that some of these eight residues are probably important for the stability of the PH domain, and thus their mutation, a deletion of all eight amino acids, may perturb functions other than just nuclear localisation. In the present study we show that mutation of just three amino acids (K487N, R489A, K493A) located on the surface of the PH domain was able to block entry of Vav1 into the nucleus, thereby more precisely defining the NLS. This more restricted mutation may be useful in defining the physiological role of Vav1 in the nucleus, about which little is currently known, though a nuclear localisation of Vav1 has been reported in several studies (Bertagnolo et al., 1998; Blanchet et al., 2005; Brugnoli et al., 2010; Clevenger et al., 1995; Romero et al., 1996; Romero et al., 1998). The dramatic change in Vav1 localisation to the nucleus in the SH3B\* point mutant suggests that this domain is binding a cytoplasmic protein, which retains Vav1 in the cytoplasm, perhaps through a canonical SH3-polyproline interaction. Alternatively, the SH3<sub>B</sub> domain may bind to sequences in Vav1 resulting in a conformation that masks the NLS, as previously suggested (Houlard et al., 2002). A 3D structure of the whole of Vav1 would help address this possibility.

Mutations in the SH2 and SH3<sub>B</sub> domains of Vav1 fully or partially inhibit its TCR-induced phosphorylation, suggesting that correct localisation of Vav1 is critical for this GEF-activating modification. The reverse possibility, that phosphorylation is required for correct localisation, is unlikely because mutation of all three tyrosine phosphorylation sites (Y142, Y160, Y174) did not affect recruitment of Vav1 to microclusters in Jurkat cells (Sylvain et al., 2011). Defective phosphorylation of the SH2\* mutant might be caused by failure of Vav1 to bind to pY315 on ZAP70 and hence to be phosphorylated by the kinase. Alternatively, the reduced phosphorylation could be caused by failure to bind to SLP76, which in turn may be required to bring Vav1 close to the kinase that phosphorylates it. In agreement with this, TCR-induced Vav1 phosphorylation is reduced in SLP76<sup>2F</sup> thymocytes (Jordan et al., 2008). Such a possibility would also explain the partial requirement for the SH3<sub>B</sub> domain, since this domain is required for high affinity binding to SLP76.

Finally, we showed that mutations in the SH2 and SH3<sub>B</sub> domains fully or partially inhibit TCR-induced calcium flux. This signalling pathway depends on Vav1 most likely because Vav1 is required for the phosphorylation of PLC $\gamma$ 1 and its subsequent activation, as judged by reduced TCR-induced IP<sub>3</sub>, a second messenger which leads to calcium flux by triggering release of calcium from intracellular stores (Fig. 6A) (Reynolds et al., 2002). We and others have shown that in primary mouse T cells this function of Vav1 is independent of its GEF activity (Miletic et al., 2009; Saveliev et al., 2009), a finding recently corroborated in Jurkat T cells (Sylvain et al., 2011). This GEF-independent function of Vav1 has been proposed to be as an adaptor protein, stabilising the binding of PLC $\gamma$ 1 to the LAT/SLP76 complex, which in turn binds the Itk kinase that phosphorylates PLC $\gamma$ 1. Our results indicate that through its SH2 domain, Vav1 binds to

SLP76, a binding that is enhanced by the SH3<sub>B</sub> domain, the same two domains that are required for a normal TCR-induced calcium flux. In view of this, we propose that the binding of Vav1 to SLP76 is critical for the TCR-induced activation of PLC $\gamma$ 1, leading to calcium flux. In agreement with our data, a recent study in Jurkat T cells also implicated the SH2 and SH3<sub>B</sub> domains in this pathway (Sylvain et al., 2011). In addition, the same study identified that the CH domain and possibly other N-terminal domains may contribute to this adaptor function for Vav1. The mechanism by which these several domains of Vav1 contribute to the activation of PLC $\gamma$ 1 is an area for future study.

In summary, we have shown that in primary mouse T cells, Vav1 is recruited to the IS and to microclusters via SLP76, we have identified domains required for this localisation and we show that this recruitment is essential for both its GEF-dependent and -independent functions.

## Materials and Methods

### Mice

Mice carrying a mutation disrupting *Vav1* (*Vav1*<sup>tm1Tyb/tm1Tyb</sup>, *Vav1*<sup>l/l</sup>) on a 129S8 or BALB/c background, or mutations in the PH (*Vav1*<sup>tm2Tyb/tm2Tyb</sup>, *Vav1*<sup>R422G/R422G</sup>) and DH (*Vav1*<sup>tm4Tyb/tm4Tyb</sup>, *Vav1*) domains of Vav1 have been described previously (Prisco et al., 2005; Saveliev et al., 2009; Turner et al., 1997). Mice carrying the Y112F,Y128F mutation in the *Lcp2* gene, which encodes for SLP76, were described previously (*SLP76*<sup>2F</sup>) (Jordan et al., 2008). Transgenic mice expressing the F5, DO11.10, 5C.C7 and P14 TCRs have been described previously (Mamalaki et al., 1993; Murphy et al., 1990; Pircher et al., 1989; Seder et al., 1992). Mice bearing the F5 and DO11.0 TCRs were crossed onto a background deficient in Rag1 (*Rag1*<sup>tm1Bal/tm1Bal</sup>) (Spanopoulou et al., 1994). All animal experiments were performed following approval by the local Ethical Review Process of the MRC National Institute for Medical Research and authorisation by the UK Home Office under relevant Project Licence authority.

### Generation of bone marrow chimeras

Bone marrow cells from C57BL/6J or SLP76<sup>2F</sup> mice were injected intravenously into C57BL/6J-*Rag1*<sup>tm1Mom/tm1Mom</sup> male mice previously irradiated with 5 Gy from a <sup>137</sup>Cs source. T cells from these mice were used 6 or more weeks after reconstitution.

### DNA constructs

To generate a fusion protein between enhanced green fluorescent protein (EGFP) and mouse Vav1, the complete open reading frame of EGFP without the stop codon was taken from pEGFP-C1 (Clontech) and joined to the 5' end of the complete mouse Vav1 cDNA including a stop codon, with a linker between the two consisting of the sequence AGTACTGGA, encoding the amino acids Ser-Thr-Gly. This EGFP-Vav1 fusion open reading frame was cloned into an *EcoRI* site in the pMSCV retroviral vector to generate pMSCV-EGFP-Vav1. Mutations in Vav1 were introduced into this construct using standard methods.

### Cell culture

To isolate F5 CD8<sup>+</sup> T cells, lymph nodes and spleens from F5 transgenic mice were mechanically disrupted, and erythrocytes were removed from splenocyte preparations by lysis with ACK buffer (0.15 M NH<sub>4</sub>Cl, 1 mM KHCO<sub>3</sub>, 0.1 mM EDTA). To induce activation, F5 T cells were cultured at a concentration of 1×10<sup>6</sup> cells/ml with 10 nM NP68 peptide for 72 h in T cell medium [RPMI-1640, 10% fetal calf serum, 10,000 U/ml penicillin, 10 mg/ml streptomycin, 2 mM L-glutamine (Sigma), non essential amino acids (Gibco), 10 mM HEPES (Gibco) and 50 μM 2-mercaptoethanol (Gibco)]. Dead cells were removed using Lympholyte-M (Cedarlane Laboratories) according to the manufacturer's protocol. Viable lymphocytes were cultured for a further 96 h at 0.2×10<sup>6</sup> cells/ml in T cell medium with 15 ng/ml IL-2 (Peprotech) after which they were used for conjugate formation experiments. DO11.10 CD4<sup>+</sup> T cells from lymph nodes were prepared as described above and activated by co-culturing 1×10<sup>6</sup> DO11.10 CD4<sup>+</sup> T cells for 72 h in T cell medium with 2×10<sup>6</sup> BALB/c splenocytes that had been previously irradiated (300 rads) and loaded with OVA<sub>323-339</sub> peptide (final concentration 0.25 μM). Subsequently, T cells (1×10<sup>6</sup> cells/ml) were cultured with IL-2 (5 ng/ml) for 96 h and used for conjugate formation experiments. CD4<sup>+</sup> T cells from wild-type, *Vav1*<sup>l/l</sup> animals or radiation chimeras reconstituted with wild-type or *SLP76*<sup>2F/2F</sup> bone marrow, were isolated from lymph nodes and purified by negative selection (Dynabeads) using anti-CD8, anti-B220 and anti-Mac1 antibodies. Purity was checked by flow cytometry and was typically in the range of 80–90%. 2×10<sup>6</sup> purified CD4<sup>+</sup> T cells were activated by plate-bound anti-CD3ε (2C11 clone) and anti-CD28 (37.51 clone) antibodies at concentration 1.5 μg/ml for WT cells

and at 3 μg/ml for *Vav1*<sup>l/l</sup> T cells for 72 h in T cell medium. Subsequently, cells were cultured (0.7–1×10<sup>6</sup> cells/ml) with IL-2 (15 ng/ml) for 96 h. *Vav1*-deficient B cells used as APCs in conjugate formation experiments, were isolated from the spleens of 129S8-*Vav1*<sup>l/l</sup> or BALB/c-*Vav1*<sup>l/l</sup> mice by negative selection (Dynabeads) using anti-CD43 and anti-TCR $\beta$  antibodies. Purity was typically 85–95%.

### Retroviral production and transduction

To produce retrovirions, the ecotropic packaging cell line PlatE (Morita et al., 2000) was transfected with DNA encoding pMSCV1-based vectors and GeneJuice (Novagen) according to the manufacturer's instructions. Supernatant from transfected cells was collected 48 h and 72 h after transfection, filtered through 0.45-μm filters to remove cell debris, concentrated by centrifugation (15,000 g, 2 h, 4°C) and resuspended in 1/10th of the original volume. Concentrated supernatants were immediately used to infect target cells or frozen and stored at –80°C for later use. T cells were transduced with retroviral vectors 24 h (F5 CD8<sup>+</sup> or CD4<sup>+</sup> BALB/c T cells) or 48 h post activation (DO11.10 CD4<sup>+</sup> T cells). CD4<sup>+</sup> BALB/c T cells were transduced in the presence of Polybrene (0.5 μg/ml). CD4<sup>+</sup> T cells were 'spinfected' by centrifugation of the cells with the concentrated viral supernatant at 2000 rpm for 1 h, whereas CD8<sup>+</sup> T cells were cultured in the presence of virus for 48 h.

### Imaging of conjugates and microclusters

Formation of T cell-APC conjugates, imaging and analysis were performed as described earlier (Saveliev et al., 2009). Cells were stained with antibodies to Vav1 (2502, Cell Signaling) and phosphotyrosine (4G10, Millipore). Polarisation of Vav1 or phosphotyrosine was calculated as a recruitment index (RI) being the ratio of mean fluorescence intensity (MFI) at the APC contact site versus the MFI of the rest of the cell. For scoring the recruitment of molecules toward the APC, positive conjugates were defined as those where the RI of the molecules in question was at least 1 standard deviation (SD) greater than the mean RI in T cells conjugated to APCs bearing no antigen. Imaging of live 5C.C7 CD4<sup>+</sup> or P14 CD8<sup>+</sup> T cells expressing EGFP-Vav1 and subsequent classification of the patterns of accumulation of EGFP-Vav1 was carried out using image processing as previously described (Singleton et al., 2009). 5C.C7 T cells were conjugated with CH27 B cell lymphoma APCs pulsed with 10 μM MCC agonist peptide. P14 T cells were conjugated with B cells from C57BL/6 mice that had been activated for 3 days with anti-CD40 (0.5 μg/ml) and pulsed with 10 μM gp33 agonist peptide.

To image microcluster formation, activated T cells were stimulated for 3 min at 37°C on coverslips (MatTek Corporation; P35G-1.5-10-C) previously coated with anti-CD3ε (2C11 clone) and in some cases also with anti-CD28 (37.51 clone) antibodies (both at 10 μg/ml). Poly-L-lysine coated coverslips were used as a negative control. Following stimulation, cells were fixed with 3% paraformaldehyde for 20 min at room temperature, washed twice with PBS, and permeabilised with 0.3% Triton X-100 in PBS for 2 min. Binding of primary and secondary antibodies was performed in blocking solution [PBS containing 0.1% saponin (Sigma, S4521) and 0.25% gelatin (Sigma, G7765)]. EGFP-Vav1 was detected using anti-GFP (chicken IgY, A10262, Invitrogen) with goat anti-chicken IgY NL493 (NL018, R&D Systems) as a secondary antibody. SLP76 was detected using an anti-SLP76 (rabbit polyclonal antibody, sc-9062, Santa Cruz) with AF568 donkey anti-rabbit Ig (A10042, Invitrogen) as a secondary antibody. TIRF imaging was carried out as previously described (Knipe et al., 2010), using an Olympus UPLSAPO×100 1.40NA objective and a custom build objective based TIRF system (Mashanov et al., 2003). Excitation light was provided by a 20 mW 488 nm laser (Point Source, Hamble UK), and a 50 mW 561 nm laser (GLC-050-561, CrystalLasers, Nevada, USA), and illumination was synchronised with image capture using WinFluor software (<http://spider.science.strath.ac.uk>). Analysis was performed using ImageJ and JACoP software. Area fraction was calculated as area of all clusters/area of cell.

### Measurement of Ca<sup>2+</sup> flux

Ca<sup>2+</sup> flux in T cells labelled with PerCP-conjugated anti-CD4, anti-CD3ε (10 μg/ml), and Indo-1 am (2 μg/ml, Molecular Probes) was measured with LSRII flow cytometers (BD Biosciences) as previously described (Reynolds et al., 2002). To measure calcium release from intracellular stores without influx across the plasma membrane, ethylene glycol-bis(2-aminoethylether)-N,N,N',N'-tetraacetic acid (EGTA, 10 mM) was added to the medium.

### Immunoprecipitation and immunoblotting

Activated T cells were rested in proliferation medium without IL-2 for 5 h. Stimulation of the cells through the TCR by cross-linking with antibodies against CD3ε (10 μg/ml) and CD28 (10 μg/ml) and subsequent immunoprecipitation and immunoblotting were performed as described earlier (Reynolds et al., 2002). Vav1 was immunoprecipitated using an antibody against Vav1 (C-14, Santa Cruz). The following antibodies were used for immunoblotting: anti-Vav1 (Cell Signaling, 2502), anti-Erk2 (sc-154, Santa Cruz Biotechnology), anti-phospho Erk2 (sc-7383, Santa Cruz Biotechnology), anti-phosphotyrosine (4G10; Upstate Biotechnology), Alexa Fluor-680 conjugated anti-mouse (Invitrogen; A21058) and IRDye800 anti-rabbit (Rockland; 611-132-122). Signals were detected with an Odyssey Infrared

Imager (Li-Cor Biotechnology) and analysed with the manufacturer's software. The degree of phosphorylation was determined as a ratio of the intensity of the bands of phosphorylated proteins to those of total proteins. Each signal was normalised to the phosphorylation signal of EGFP-Vav1 at 1 min, which was set to 100% and multiple experiments were combined to generate mean  $\pm$  SEM.

#### Expression and purification of recombinant proteins and isothermal titration calorimetry (ITC)

Recombinant fragments of mouse Vav1 were expressed in *E. coli*. The SH2 domain (669–771) was expressed at 16°C as a GST fusion from pGEX-6P1 (GE Life Sciences), purified by GST affinity chromatography. After removal of the GST-tag by PreScission Protease the protein was purified to homogeneity by gel filtration. SH3A-SH2 (596–771) and SH2-SH3B (669–845) were expressed at 37°C from pET28a (Novagen) with a His<sub>6</sub>-tag, and purified by nickel affinity and gel filtration chromatography according to standard protocols. SH3-SH2-SH3B (596–845) was expressed in a modified pET22b vector containing a biotinylation site preceded by a PreScission Protease site at the C-terminus of the protein. The protein was bound to streptavidin-coated beads (Pierce), incubated overnight with protease and purified to homogeneity by gel filtration. All gel filtration was carried out in ITC buffer (20 mM Hepes pH 7.5, 150 mM NaCl, 1 mM EDTA, 1 mM TCEP), which was also used to re-suspend the peptides. Protein and peptide concentrations were determined by absorbance at 280 nm. Peptides were synthesised by W. Mawby, University of Bristol and contained the following sequences: pY112: EDDpYESPND, pY128: DGDpYESPNE and 2pY:EDDpYESPNDGDDGDDGpYESPNE. ITC experiments were performed at 20°C using an ITC-200 calorimeter (GE Life Sciences). Heats of dilution were subtracted from the raw ITC data prior to analysis with the software, Micro Origin version 7.0, assuming a single-site binding model.

#### Statistical analysis

All statistical comparisons were carried out using the nonparametric two-tailed Mann–Whitney test, an unpaired two-tailed *t*-test, or Fisher's exact test. Statistically significant differences are indicated on the figures: \**P*<0.05, \*\**P*<0.01, \*\*\**P*<0.001.

#### Acknowledgements

We thank Agnieszka Zachacz for expert assistance, Edina Schweighoffer for help in generation of chimeric mice and Daniel Billadeau, Steve Smerdon and Gary Koretzky for advice.

#### Funding

M.F. was a recipient of an EMBO long-term fellowship (fellowship number ALTF 508-2005) and a EU Marie Curie fellowship. (fellowship number EIF 025449). O.K., A.S., J.R., K.R., T.C. and V.T. were funded by the UK Medical Research Council programme [grant numbers U117527252, U117565398 and U117573808]; R.K. was supported by Wellcome Trust [grant number 089185]. Deposited in PMC for immediate release.

Supplementary material available online at

<http://jcs.biologists.org/lookup/suppl/doi:10.1242/jcs.105148/-/DC1>

#### References

- Aghazadeh, B., Lowry, W. E., Huang, X. Y. and Rosen, M. K. (2000). Structural basis for relief of autoinhibition of the Dbl homology domain of proto-oncogene Vav by tyrosine phosphorylation. *Cell* **102**, 625–633.
- Ardouin, L., Bracke, M., Mathiot, A., Pagakis, S. N., Norton, T., Hogg, N. and Tybulewicz, V. L. J. (2003). Vav1 transduces TCR signals required for LFA-1 function and cell polarization at the immunological synapse. *Eur. J. Immunol.* **33**, 790–797.
- Barda-Saad, M., Braiman, A., Titerence, R., Bunnell, S. C., Barr, V. A. and Samelson, L. E. (2005). Dynamic molecular interactions linking the T cell antigen receptor to the actin cytoskeleton. *Nat. Immunol.* **6**, 80–89.
- Barda-Saad, M., Shirasu, N., Pauker, M. H., Hassan, N., Perl, O., Balbo, A., Yamaguchi, H., Houtman, J. C., Appella, E., Schuck, P. et al. (2010). Cooperative interactions at the SLP-76 complex are critical for actin polymerization. *EMBO J.* **29**, 2315–2328.
- Beal, A. M., Anikeeva, N., Varma, R., Cameron, T. O., Vasiliver-Shamis, G., Norris, P. J., Dustin, M. L. and Sykulev, Y. (2009). Kinetics of early T cell receptor signaling regulate the pathway of lytic granule delivery to the secretory domain. *Immunity* **31**, 632–642.
- Bertagnolo, V., Marchisio, M., Volinia, S., Caramelli, E. and Capitani, S. (1998). Nuclear association of tyrosine-phosphorylated Vav to phospholipase C- $\gamma$ 1 and phosphoinositide 3-kinase during granulocytic differentiation of HL-60 cells. *FEBS Lett.* **441**, 480–484.
- Blanchet, F., Cardona, A., Letimier, F. A., Hershfield, M. S. and Acuto, O. (2005). CD28 costimulatory signal induces protein arginine methylation in T cells. *J. Exp. Med.* **202**, 371–377.
- Braiman, A., Barda-Saad, M., Sommers, C. L. and Samelson, L. E. (2006). Recruitment and activation of PLC $\gamma$ 1 in T cells: a new insight into old domains. *EMBO J.* **25**, 774–784.
- Brunoli, F., Lambertini, E., Varin-Blank, N., Piva, R., Marchisio, M., Grassilli, S., Miscia, S., Capitani, S. and Bertagnolo, V. (2010). Vav1 and PU.1 are recruited to the CD11b promoter in APL-derived promyelocytes: role of Vav1 in modulating PU.1-containing complexes during ATRA-induced differentiation. *Exp. Cell Res.* **316**, 38–47.
- Bunnell, S. C., Diehn, M., Yaffe, M. B., Findell, P. R., Cantley, L. C. and Berg, L. J. (2000). Biochemical interactions integrating Itk with the T cell receptor-initiated signaling cascade. *J. Biol. Chem.* **275**, 2219–2230.
- Bunnell, S. C., Kapoor, V., Tribble, R. P., Zhang, W. and Samelson, L. E. (2001). Dynamic actin polymerization drives T cell receptor-induced spreading: a role for the signal transduction adaptor LAT. *Immunity* **14**, 315–329.
- Bunnell, S. C., Hong, D. L., Kardon, J. R., Yamazaki, T., McClade, C. J., Barr, V. A. and Samelson, L. E. (2002). T cell receptor ligation induces the formation of dynamically regulated signaling assemblies. *J. Cell Biol.* **158**, 1263–1275.
- Bunnell, S. C., Singer, A. L., Hong, D. L., Jacque, B. H., Jordan, M. S., Seminario, M.-C., Barr, V. A., Koretzky, G. A. and Samelson, L. E. (2006). Persistence of cooperatively stabilized signaling clusters drives T-cell activation. *Mol. Cell Biol.* **26**, 7155–7166.
- Campi, G., Varma, R. and Dustin, M. L. (2005). Actin and agonist MHC-peptide complex-dependent T cell receptor microclusters as scaffolds for signaling. *J. Exp. Med.* **202**, 1031–1036.
- Chrencik, J. E., Brooun, A., Zhang, H., Mathews, I. L., Hura, G. L., Foster, S. A., Perry, J. J., Streiff, M., Ramage, P., Widmer, H. et al. (2008). Structural basis of guanine nucleotide exchange mediated by the T-cell essential Vav1. *J. Mol. Biol.* **380**, 828–843.
- Clevenger, C. V., Ngo, W., Sokol, D. L., Luger, S. M. and Gewirtz, A. M. (1995). Vav is necessary for prolactin-stimulated proliferation and is translocated into the nucleus of a T-cell line. *J. Biol. Chem.* **270**, 13246–13253.
- Costello, P. S., Walters, A. E., Mee, P. J., Turner, M., Reynolds, L. F., Prisco, A., Sarner, N., Zamoyska, R. and Tybulewicz, V. L. J. (1999). The Rho-family GTP exchange factor Vav is a critical transducer of T cell receptor signals to the calcium, ERK, and NF- $\kappa$ B pathways. *Proc. Natl. Acad. Sci. USA* **96**, 3035–3040.
- Dombroski, D., Houghtling, R. A., Labno, C. M., Precht, P., Takesono, A., Caplen, N. J., Billadeau, D. D., Wange, R. L., Burkhardt, J. K. and Schwartzberg, P. L. (2005). Kinase-independent functions for Itk in TCR-induced regulation of Vav and the actin cytoskeleton. *J. Immunol.* **174**, 1385–1392.
- Dustin, M. L., Olszowy, M. W., Holdorf, A. D., Li, J., Bromley, S., Desai, N., Widder, P., Rosenberger, F., van der Merwe, P. A., Allen, P. M. et al. (1998). A novel adaptor protein orchestrates receptor patterning and cytoskeletal polarity in T-cell contacts. *Cell* **94**, 667–677.
- Dustin, M. L., Chakraborty, A. K. and Shaw, A. S. (2010). Understanding the structure and function of the immunological synapse. *Cold Spring Harb. Perspect. Biol.* **2**, a002311.
- Fang, N. and Koretzky, G. A. (1999). SLP-76 and Vav function in separate, but overlapping pathways to augment interleukin-2 promoter activity. *J. Biol. Chem.* **274**, 16206–16212.
- Fischer, K.-D., Kong, Y.-Y., Nishina, H., Tedford, K., Marengère, L. E. M., Koziaradzki, I., Sasaki, T., Starr, M., Chan, G., Gardener, S. et al. (1998). Vav is a regulator of cytoskeletal reorganization mediated by the T-cell receptor. *Curr. Biol.* **8**, 554–562.
- Grakoui, A., Bromley, S. K., Sumen, C., Davis, M. M., Shaw, A. S., Allen, P. M. and Dustin, M. L. (1999). The immunological synapse: a molecular machine controlling T cell activation. *Science* **285**, 221–227.
- Groisman, M., Hornstein, I., Alcover, A. and Katzav, S. (2002). Vav1 and Ly-GDI two regulators of Rho GTPases, function cooperatively as signal transducers in T cell antigen receptor-induced pathways. *J. Biol. Chem.* **277**, 50121–50130.
- Han, J., Luby-Phelps, K., Das, B., Shu, X., Xia, Y., Mosteller, R. D., Krishna, U. M., Falck, J. R., White, M. A. and Broek, D. (1998). Role of substrates and products of PI 3-kinase in regulating activation of Rac-related guanosine triphosphatases by Vav. *Science* **279**, 558–560.
- Holsinger, L. J., Graef, I. A., Swat, W., Chi, T., Bautista, D. M., Davidson, L., Lewis, R. S., Alt, F. W. and Crabtree, G. R. (1998). Defects in actin-cap formation in Vav-deficient mice implicate an actin requirement for lymphocyte signal transduction. *Curr. Biol.* **8**, 563–572.
- Houlard, M., Arudchandran, R., Regnier-Ricard, F., Germani, A., Gisselbrecht, S., Blank, U., Rivera, J. and Varin-Blank, N. (2002). Vav1 is a component of transcriptionally active complexes. *J. Exp. Med.* **195**, 1115–1127.
- Jenkins, M. R., Tsun, A., Stinchcombe, J. C. and Griffiths, G. M. (2009). The strength of T cell receptor signal controls the polarization of cytotoxic machinery to the immunological synapse. *Immunity* **31**, 621–631.
- Jordan, M. S., Smith, J. E., Burns, J. C., Austin, J. E., Nichols, K. E., Aschenbrenner, A. C. and Koretzky, G. A. (2008). Complementation in trans of altered thymocyte development in mice expressing mutant forms of the adaptor molecule SLP76. *Immunity* **28**, 359–369.
- Katzav, S., Sutherland, M., Packham, G., Yi, T. and Weiss, A. (1994). The protein tyrosine kinase ZAP-70 can associate with the SH2 domain of proto-Vav. *J. Biol. Chem.* **269**, 32579–32585.

- Knipe, L., Meli, A., Hewlett, L., Bierings, R., Dempster, J., Skehel, P., Hannah, M. J. and Carter, T. (2010). A revised model for the secretion of tPA and cytokines from cultured endothelial cells. *Blood* **116**, 2183-2191.
- Koretzky, G. A., Abtahian, F. and Silverman, M. A. (2006). SLP76 and SLP65: complex regulation of signalling in lymphocytes and beyond. *Nat. Rev. Immunol.* **6**, 67-78.
- Krawczyk, C., Oliveira-dos-Santos, A., Sasaki, T., Griffiths, E., Ohashi, P. S., Snapper, S., Alt, F. and Penninger, J. M. (2002). Vav1 controls integrin clustering and MHC/peptide-specific cell adhesion to antigen-presenting cells. *Immunity* **16**, 331-343.
- Lemmon, M. A. (2008). Membrane recognition by phospholipid-binding domains. *Nat. Rev. Mol. Cell Biol.* **9**, 99-111.
- Mamalak, C., Elliott, J., Norton, T., Yannoutsos, N., Townsend, A. R., Chandler, P., Simpson, E. and Kiousis, D. (1993). Positive and negative selection in transgenic mice expressing a T-cell receptor specific for influenza nucleoprotein and endogenous superantigen. *Dev. Immunol.* **3**, 159-174.
- Mashanov, G. I., Tacon, D., Knight, A. E., Peckham, M. and Molloy, J. E. (2003). Visualizing single molecules inside living cells using total internal reflection fluorescence microscopy. *Methods* **29**, 142-152.
- Michel, F., Mangino, G., Attal-Bonnefoy, G., Tuosto, L., Alcover, A., Roumier, A., Olive, D. and Acuto, O. (2000). CD28 utilizes Vav-1 to enhance TCR-proximal signaling and NF-AT activation. *J. Immunol.* **165**, 3820-3829.
- Miletic, A. V., Sakata-Sogawa, K., Hiroshima, M., Hamann, M. J., Gomez, T. S., Ota, N., Kloepfel, T., Kanagawa, O., Tokunaga, M., Billadeau, D. D. et al. (2006). Vav1 acidic region tyrosine 174 is required for the formation of T cell receptor-induced microclusters and is essential in T cell development and activation. *J. Biol. Chem.* **281**, 38257-38265.
- Miletic, A. V., Graham, D. B., Sakata-Sogawa, K., Hiroshima, M., Hamann, M. J., Cemerski, S., Kloepfel, T., Billadeau, D. D., Kanagawa, O., Tokunaga, M. et al. (2009). Vav links the T cell antigen receptor to the actin cytoskeleton and T cell activation independently of intrinsic Guanine nucleotide exchange activity. *PLoS ONE* **4**, e6599.
- Monks, C. R. F., Freiberg, B. A., Kupfer, H., Sciaky, N. and Kupfer, A. (1998). Three-dimensional segregation of supramolecular activation clusters in T cells. *Nature* **395**, 82-86.
- Morita, S., Kojima, T. and Kitamura, T. (2000). Plat-E: an efficient and stable system for transient packaging of retroviruses. *Gene Ther.* **7**, 1063-1066.
- Mossman, K. D., Campi, G., Groves, J. T. and Dustin, M. L. (2005). Altered TCR signaling from geometrically repatterned immunological synapses. *Science* **310**, 1191-1193.
- Murphy, K. M., Heimerlinger, A. B. and Loh, D. Y. (1990). Induction by antigen of intrathymic apoptosis of CD4+CD8+TCR $\alpha$  thymocytes in vivo. *Science* **250**, 1720-1723.
- Nishida, M., Nagata, K., Hachimori, Y., Horiuchi, M., Ogura, K., Mandiyan, V., Schlessinger, J. and Inagaki, F. (2001). Novel recognition mode between Vav and Grb2 SH3 domains. *EMBO J.* **20**, 2995-3007.
- Nunes, J. A., Battifora, M., Woodgett, J. R., Truneh, A., Olive, D. and Cantrell, D. A. (1996). CD28 signal transduction pathways. A comparison of B7-1 and B7-2 regulation of the map kinases: ERK2 and Jun kinases. *Mol. Immunol.* **33**, 63-70.
- O'Keefe, J. P., Blaine, K., Alegre, M. L. and Gajewski, T. F. (2004). Formation of a central supramolecular activation cluster is not required for activation of naive CD8+ T cells. *Proc. Natl. Acad. Sci. USA* **101**, 9351-9356.
- Pircher, H., Bürki, K., Lang, R., Hengartner, H. and Zinkernagel, R. M. (1989). Tolerance induction in double specific T-cell receptor transgenic mice varies with antigen. *Nature* **342**, 559-561.
- Prisco, A., Vanes, L., Ruf, S., Trigueros, C. and Tybulewicz, V. L. J. (2005). Lineage-specific requirement for the PH domain of Vav1 in the activation of CD4+ but not CD8+ T cells. *Immunity* **23**, 263-274.
- Raab, M., Pfister, S. and Rudd, C. E. (2001). CD28 signaling via VAV/SLP-76 adaptors: regulation of cytokine transcription independent of TCR ligation. *Immunity* **15**, 921-933.
- Rapley, J., Tybulewicz, V. L. and Rittinger, K. (2008). Crucial structural role for the PH and CI domains of the Vav1 exchange factor. *EMBO Rep.* **9**, 655-661.
- Reynolds, L. F., Smyth, L. A., Norton, T., Freshney, N., Downward, J., Kiousis, D. and Tybulewicz, V. L. J. (2002). Vav1 transduces T cell receptor signals to the activation of phospholipase C- $\gamma$ 1 via phosphoinositide 3-kinase-dependent and -independent pathways. *J. Exp. Med.* **195**, 1103-1114.
- Reynolds, L. F., de Bettignies, C., Norton, T., Beeser, A., Chernoff, J. and Tybulewicz, V. L. J. (2004). Vav1 transduces T cell receptor signals to the activation of the Ras/ERK pathway via LAT, Sos, and RasGRP1. *J. Biol. Chem.* **279**, 18239-18246.
- Romero, F., Dargemont, C., Pozo, F., Reeves, W. H., Camonis, J., Gisselbrecht, S. and Fischer, S. (1996). p95vav associates with the nuclear protein Ku-70. *Mol. Cell. Biol.* **16**, 37-44.
- Romero, F., Germani, A., Puvion, E., Camonis, J., Varin-Blank, N., Gisselbrecht, S. and Fischer, S. (1998). Vav binding to heterogeneous nuclear ribonucleoprotein (hnRNP) C. Evidence for Vav-hnRNP interactions in an RNA-dependent manner. *J. Biol. Chem.* **273**, 5923-5931.
- Saveliev, A., Vanes, L., Ksionda, O., Rapley, J., Smerdon, S. J., Rittinger, K. and Tybulewicz, V. L. (2009). Function of the nucleotide exchange activity of vav1 in T cell development and activation. *Sci. Signal.* **2**, ra83.
- Seder, R. A., Paul, W. E., Davis, M. M. and Fazekas de St Groth, B. (1992). The presence of interleukin 4 during in vitro priming determines the lymphokine-producing potential of CD4+ T cells from T cell receptor transgenic mice. *J. Exp. Med.* **176**, 1091-1098.
- Singleton, K. L., Roybal, K. T., Sun, Y., Fu, G., Gascoigne, N. R., van Oers, N. S. and Wülfing, C. (2009). Spatiotemporal patterning during T cell activation is highly diverse. *Sci. Signal.* **2**, ra15.
- Singleton, K. L., Gosh, M., Dandekar, R. D., Au-Yeung, B. B., Ksionda, O., Tybulewicz, V. L., Altman, A., Fowell, D. J. and Wülfing, C. (2011). Itk controls the spatiotemporal organization of T cell activation. *Sci. Signal.* **4**, ra66.
- Songyang, Z., Shoelson, S. E., McGlade, J., Olivier, P., Pawson, T., Bustelo, X. R., Barbacid, M., Sabe, H., Hanafusa, H., Yi, T. et al. (1994). Specific motifs recognized by the SH2 domains of Csk, 3BP2, fps/fes, GRB-2, HCP, SHC, Syk, and Vav. *Mol. Cell. Biol.* **14**, 2777-2785.
- Spanopoulou, E., Roman, C. A., Corcoran, L. M., Schlessel, M. S., Silver, D. P., Nemaze, D., Nussenzweig, M. C., Shinton, S. A., Hardy, R. R. and Baltimore, D. (1994). Functional immunoglobulin transgenes guide ordered B-cell differentiation in Rag-1-deficient mice. *Genes Dev.* **8**, 1030-1042.
- Stinchcombe, J. C., Bossi, G., Booth, S. and Griffiths, G. M. (2001). The immunological synapse of CTL contains a secretory domain and membrane bridges. *Immunity* **15**, 751-761.
- Sylvain, N. R., Nguyen, K. and Bunnell, S. C. (2011). Vav1-mediated scaffolding interactions stabilize SLP-76 microclusters and contribute to antigen-dependent T cell responses. *Sci. Signal.* **4**, ra14.
- Tamir, A., Eisenbraun, M. D., Garcia, G. G. and Miller, R. A. (2000). Age-dependent alterations in the assembly of signal transduction complexes at the site of T cell/APC interaction. *J. Immunol.* **165**, 1243-1251.
- Tuosto, L., Michel, F. and Acuto, O. (1996). p95vav associates with tyrosine-phosphorylated SLP-76 in antigen-stimulated T cells. *J. Exp. Med.* **184**, 1161-1166.
- Turner, M., Mee, P. J., Walters, A. E., Quinn, M. E., Mellor, A. L., Zamoyska, R. and Tybulewicz, V. L. J. (1997). A requirement for the Rho-family GTP exchange factor Vav in positive and negative selection of thymocytes. *Immunity* **7**, 451-460.
- Tybulewicz, V. L. J. (2005). Vav-family proteins in T-cell signalling. *Curr. Opin. Immunol.* **17**, 267-274.
- Varma, R., Campi, G., Yokosuka, T., Saito, T. and Dustin, M. L. (2006). T cell receptor-proximal signals are sustained in peripheral microclusters and terminated in the central supramolecular activation cluster. *Immunity* **25**, 117-127.
- Villalba, M., Bi, K., Rodriguez, F., Tanaka, Y., Schoenberger, S. and Altman, A. (2001). Vav1/Rac-dependent actin cytoskeleton reorganization is required for lipid raft clustering in T cells. *J. Cell Biol.* **155**, 331-338.
- Wu, J., Motto, D. G., Koretzky, G. A. and Weiss, A. (1996). Vav and SLP-76 interact and functionally cooperate in IL-2 gene activation. *Immunity* **4**, 593-602.
- Wu, J., Zhao, Q., Kurosaki, T. and Weiss, A. (1997). The Vav binding site (Y315) in ZAP-70 is critical for antigen receptor-mediated signal transduction. *J. Exp. Med.* **185**, 1877-1882.
- Wülfing, C., Bauch, A., Crabtree, G. R. and Davis, M. M. (2000). The vav exchange factor is an essential regulator in actin-dependent receptor translocation to the lymphocyte-antigen-presenting cell interface. *Proc. Natl. Acad. Sci. USA* **97**, 10150-10155.
- Xavier, R., Brennan, T., Li, Q., McCormack, C. and Seed, B. (1998). Membrane compartmentation is required for efficient T cell activation. *Immunity* **8**, 723-732.
- Yokosuka, T., Sakata-Sogawa, K., Kobayashi, W., Hiroshima, M., Hashimoto-Tane, A., Tokunaga, M., Dustin, M. L. and Saito, T. (2005). Newly generated T cell receptor microclusters initiate and sustain T cell activation by recruitment of Zap70 and SLP-76. *Nat. Immunol.* **6**, 1253-1262.
- Yu, B., Martins, I. R., Li, P., Amarasinghe, G. K., Umetani, J., Fernandez-Zapico, M. E., Billadeau, D. D., Machius, M., Tomchick, D. R. and Rosen, M. K. (2010). Structural and energetic mechanisms of cooperative autoinhibition and activation of Vav1. *Cell* **140**, 246-256.
- Zeng, R., Cannon, J. L., Abraham, R. T., Way, M., Billadeau, D. D., Bubeck-Wardenberg, J. and Burkhardt, J. K. (2003). SLP-76 coordinates Nck-dependent Wiskott-Aldrich syndrome protein recruitment with Vav-1/Cdc42-dependent Wiskott-Aldrich syndrome protein activation at the T cell-APC contact site. *J. Immunol.* **171**, 1360-1368.
- Zhang, W., Tribble, R. P. and Samelson, L. E. (1998). LAT palmitoylation: its essential role in membrane microdomain targeting and tyrosine phosphorylation during T cell activation. *Immunity* **9**, 239-246.